

Aberystwyth University

Application of symmetry law in numerical modeling of hydraulic fracturing by finite element method

Sun, Shanhui; Zhou, Meihua; Lu, Wei; Davarpanah, Afshin

Published in:
Symmetry

DOI:
[10.3390/sym12071122](https://doi.org/10.3390/sym12071122)

Publication date:
2020

Citation for published version (APA):

Sun, S., Zhou, M., Lu, W., & Davarpanah, A. (2020). Application of symmetry law in numerical modeling of hydraulic fracturing by finite element method. *Symmetry*, 12(7), [1122]. <https://doi.org/10.3390/sym12071122>

Document License CC BY

General rights

Copyright and moral rights for the publications made accessible in the Aberystwyth Research Portal (the Institutional Repository) are retained by the authors and/or other copyright owners and it is a condition of accessing publications that users recognise and abide by the legal requirements associated with these rights.

- Users may download and print one copy of any publication from the Aberystwyth Research Portal for the purpose of private study or research.
- You may not further distribute the material or use it for any profit-making activity or commercial gain
- You may freely distribute the URL identifying the publication in the Aberystwyth Research Portal

Take down policy

If you believe that this document breaches copyright please contact us providing details, and we will remove access to the work immediately and investigate your claim.

tel: +44 1970 62 2400
email: is@aber.ac.uk

Article

Application of Symmetry Law in Numerical Modeling of Hydraulic Fracturing by Finite Element Method

Shanhui Sun ^{1,2}, Meihua Zhou ^{2,*}, Wei Lu ¹ and Afshin Davarpanah ^{3,*} 

¹ College of Mathematics and Statistics, Suzhou University, Suzhou 215006, China; Sh.sun@163.com (S.S.); Lu.wei12@163.com (W.L.)

² School of Management, China University of Mining and Technology, Xuzhou 221116, China

³ Department of Mathematics, Aberystwyth University, Penglais Hill, Aberystwyth SY23 3FL, UK

* Correspondence: jkjbfg8@163.com (M.Z.); afd6@aber.ac.uk (A.D.)

Received: 8 May 2020; Accepted: 6 July 2020; Published: 6 July 2020



Abstract: In this paper, influential parameters on the hydraulic fracturing processes in porous media were investigated. Besides, the simultaneous stimulation of solids, fluids and fractures geomechanical equations were numerically analyzed as a developed 3D model. To do this, the Abacus software was used as a multi-objective program to solve the physical-mechanical symmetry law governing equations, according to the finite element method. Two different layers, A (3104–2984 m) and B (4216–4326 m), are considered in the model. According to the result of this study, the maximum fracture opening length in the connection of the wall surface is 10 and 9 mm for layer B and layer A, respectively. Moreover, the internal fracture fluid pressure for layer B and layer A is 65 and 53 Mpa. It is indicated that fracture fluid pressure reduced with the increase in fracture propagation length. Consequently, the results of this study would be of benefit for petroleum industries to consider several crucial geomechanical characteristics in hydraulic fractures simultaneously as a developed numerical model for different formation layers to compare a comprehensive analysis between each layer.

Keywords: hydraulic fracturing; symmetry law; finite element method; Abacus software; internal fracture fluid pressure

1. Introduction

Nowadays, due to the high production rate of hydrocarbons, most reservoirs are facing pressure reduction and consequently, low recovery rate [1–7]. Due to the high cost requirement for crude oil treatment as well as environmental considerations, it is vital to assess and anticipate some matters before the primary treatment. It is particularly related to the geometry of the induced fractures and the pressures that are required for initiation and propagation of the fractures alike [8–13]. Hydrofracturing is considered as one of the crucial processes in geological concepts, especially for the upper crust deformation. The reason of hydrofracturing administration is to produce permeable pore spaces and throats, which has caused the mobilization of more hydrocarbon volume toward the production wells [12,14–16]. Flekkøy et al. [17] developed a numerical model to evaluate the hydraulic fracturing performances by the utilization of fluid pressure diffusion and discrete spring network. Regarding the lack of redundant components in fluid dynamics description, their developed model was efficient and versatile to consider generic impacts of simple geological scenarios. They found that fracture deformation is utterly dependent on the rock pressure diffusion and elastic continuum limit to determine appropriate macroscopic factors [17]. The problem of hydraulic rupture is a three-dimensional problem, which is used to determine the opening (width), length and height of the fracture [16,18–20]. Rupture is known as one of the immediate failure processes along a fault that can eliminate seismic waves which should be taken into consideration in recent decades in geological

structures. Furthermore, faults' stick-slip behavior is considered as a substantial parameter in rupture recognition [21].

Al-Busaidi et al. [22] investigated the fracture propagation and development mechanisms in hydraulic fracturing processes by the administration of a discrete particle discontinuum method. The proposed model is based on the individual structures' breakage and separate particles contact points. They concluded that the dominant mechanisms of induced hydrofracture are shear cracks and tensile failure [22]. Ghani et al. [23] proposed a numerical model to analytically model the natural hydrofracture dynamic development by the utilization of the discrete element method. It is based on Darcy pore pressure diffusion. This model could provide a porosity-controlled model that is associated between the hydraulic field and fractured network. They concluded that seepage forces that are made by discrete fracturing poroelastic forces associated with pressure gradients in the hydraulic situation would play a substantial role in rock deformation of underground formations. The reason for this issue is that tectonic stresses, hydrofracture geometry, and porous rocks' mechanical characteristics are being changed by these forces [23]. Field information on hydraulic fracturing operations is mainly available as pressure-time curves. It is not possible to determine the actual geometry of a hydraulic fracture using this information alone [7,24–26]. Therefore, design and control of hydraulic fracturing operations are possible only by relying on mathematical models and sophisticated numerical methods [27–29].

There are two general methods—boundary methods and areal methods—to model rock behavior in porous media. Boundary methods are considered as those methods in which only the drilling boundary is divided into small components, and rock bulk volume is just an infinite continuous region. Areal methods are those methods that bulk phases of rock are divided into small geometric sections. It is assumed that each section has similar properties. Different types of numerical methods in rock engineering are schematically depicted in Figure 1.

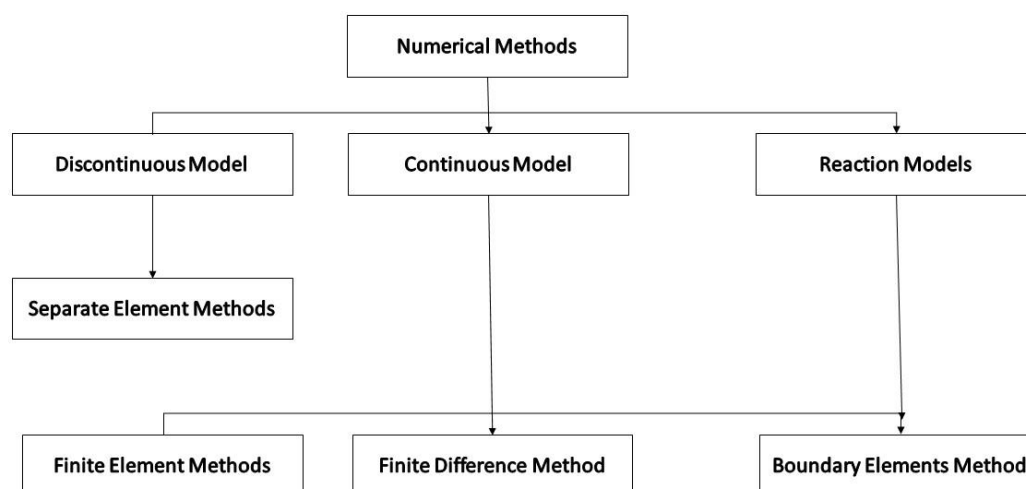


Figure 1. Numerical methods in rock engineering.

Liu et al. [30] proposed a numerical model based on the extended finite element method and hybrid finite volume to simulate the propagation of hydraulic fracturing. It is coupled with the fluid flow and rock deformation behavior as the one-dimensional flow for the laminar condition. To analyze the nonlinear fractures, the cohesive crack model was used as it is more adapted with the reservoir characteristics in the real condition [30]. Zhang et al. [31] proposed a developed discrete element method coupled with a synthetic rock mass method to model the fluid-driven fracture propagation. To do this, five different samples for different conditions of induced seismicity, in-fill well fracturing, multi-stage hydraulic fracturing, near-wellbore tortuosity and fracture initiation, and hydraulic fracture interaction were investigated. They concluded that the developed model would be a qualitative model to simulate hydraulic fracturing processes under several uncertainties [31].

Zheng et al. [32] investigated the bedding plane effect on the fracture propagation by the finite-discrete element method. In this model, by developing a complex fracture network, fracturing fluid leakage and low net pressure in bedding planes were numerically analyzed. They found that developing the mixed fracturing method to enhance the volume of the stimulated reservoir is the privilege of this model than the fracture network generation alone [32]. He et al. [33] proposed a numerical model to consider the microscopic heterogeneity impact on the fracture behavior in hydraulic fracturing processes in porous media. In this model, the phase-field fracture modeling method was used. It was combined with the homogenization technique to investigate the heterogeneity impact. Homogenized elasticity tensor was computed in the model regarding the boundary value problems solution and the macroscopic fractures' subsequent propagation. Besides, strain energy was calculated accordingly in the proposed model. They concluded that the propagation path and fracture strength would be impacted by microscopic heterogeneity in underlying pore structure during hydraulic fracturing processes [33]. Alotaibi et al. [34] developed a numerical model to couple the fracture mechanics through the cracks and porous media by the simulation of Darcy type flow as the Stokes type flow in open cracks. Furthermore, they used the phase-field fracture modeling method to consider the interactions between material interfaces when there is fluid driven force on the cracks. According to their results, layer elasticity modulus versus matrix will not be a crucial parameter to create barriers in the fracture toughness. Moreover, there is a lower fracture deflect tendency during the steep orientation in the crack direction. Furthermore, the distance of layer and injection point did not play the primary role in fracture deflecting [34].

Lack of a precise model due to the different reservoir heterogeneity and geomechanical properties of the reservoir in each specific condition had posed severe challenges for petroleum industries in operational performances. Therefore, the creation of a three-dimensional numerical model that simultaneously considers the mechanical equations of solids, fluids and fractures are one of the primary objectives of this research. This study aimed to simulate these influential parameters as a developed 3D numerical model in hydraulic fracturing procedure. To do this, modeling was performed by assuming limitations and solving the governing equations by the Abacus software as a multi-objective program for modeling physical and mechanical reservoir properties in porous media according to the finite element method. This simulation includes geostatic steps and fluid injection into the well, which will lead to the onset of hydraulic fractures. Finally, this model would be used to simulate reservoirs with different geomechanical characteristics by determining the onset and propagation of fracture versus pressure and time for different layers.

2. Materials and Methods

2.1. Governing Equations

To model hydraulic fracturing process, five dependent phenomena of porous medium deformation, pore fluid flow, fracturing fluid flow, fracture initiation and propagation should be coupled and numerically analyzed. The porous medium can be modeled as a homogeneous poroelastic material that has undergone a pseudo-static deformation. The governing equations are based on the symmetry law, as considering tortuous fractures in the modeling processes would be more complicated. The equilibrium equation when volumetric forces are ignored:

$$\sigma_{ij,j} = 0 \quad (1)$$

While the structural relationship of poroelastic, assuming small strains, is equal to:

$$\sigma_{ij} - \sigma_{ij}^0 = 2G\varepsilon_{ij} + (K - \frac{2}{3}G)\varepsilon_{kk} - \alpha(p - p_0)\delta_{ij} \quad (2)$$

$$2G = \frac{E}{1 + \nu} \quad (3)$$

$$3K = \frac{E}{(1-2\nu)} \quad (4)$$

In which σ is the Biot coefficient, G and K are the shear elasticity and shear bulk modulus, E is the Yang modulus, and ν is the Poisson ratio for the dry state, respectively. Using the Terzaghi effective stresses law, the above equations can be written in terms of stress and effective strain as follows [35]:

$$\sigma'_{ij} = \sigma_{ij} + p\delta_{ij} \quad (5)$$

$$\sigma'_{ij} - \sigma'^0_{ij} = 2G\varepsilon'_{ij} + (K - \frac{2}{3}G)\varepsilon'_{kk}\delta_{ij} \quad (6)$$

$$\varepsilon'_{ij} = \varepsilon - \frac{\alpha-1}{3K}(p-p_0)\delta_{ij} \quad (7)$$

Continuity equation for pore fluid flow assuming small volumetric strains, it is equal to:

$$\frac{1}{M}\rho_{k,k} + \sigma\varepsilon_{k,k} + V_{k,k} = 0 \quad (8)$$

where V_k is the velocity of pore fluid flow, M and σ are the Biot modulus and Biot's coefficient, respectively. Two fixed poroelastic constants are defined as follows:

$$\frac{1}{M} = \frac{\phi_0}{K_f} + \frac{\alpha - \phi_0}{K_s} \quad (9)$$

$$\frac{1}{K_s} = \frac{1 - \alpha}{K} \quad (10)$$

where K_f is the perforated bulk modulus, K_s is the solid grains modulus in a porous medium, and ϕ is the initial porosity. It is assumed that the permeable fluid will flow through an interconnected permeable network according to Darcy's law:

$$V_i = -\frac{k}{\mu}p_{,i} = -\frac{\bar{k}}{\gamma}p_{,i} \quad (11)$$

where k is permeability, μ is pore fluid viscosity, \bar{k} is hydraulic conductivity and γ is the specific gravity of pore fluid. By combining Equation (11) with the continuity equation (Equation (8)), the equation for propagating the pore fluid is obtained from the following equation:

$$\frac{1}{M}\rho + \alpha\varepsilon_{k,k} = \frac{\bar{k}}{\gamma}p_{k,k} \quad (12)$$

The hydraulic fracturing fluid flow is defined according to Reynolds' theory, which dominates the flow of longitudinal fluid within the fracture as follows:

$$g + \frac{\partial q_f}{\partial s} + V_T + V_B = 0 \quad (13)$$

The flow equation for incompressible and Newtonian fluids through parallel thin plates (e.g., Poiseuille flow) as follows:

$$q_f = -\frac{g^3}{12\mu_f} \frac{\partial p_f}{\partial s} \quad (14)$$

where g is the fracture distance (Figure 1), $g_f = V_f g$ hydraulic fracturing fluid flow (per width) across the fracture, V_T and V_B are the normal (vertical) velocity of the hydraulic fracturing fluid that penetrates the porous medium through the upper and lower fracture surfaces. μ_f is the hydraulic fracturing fluid

velocity and p_f fluid pressure along the fracture surface, which is marked with the characteristics of the linear curve, s . It is schematically depicted in Figure 2.

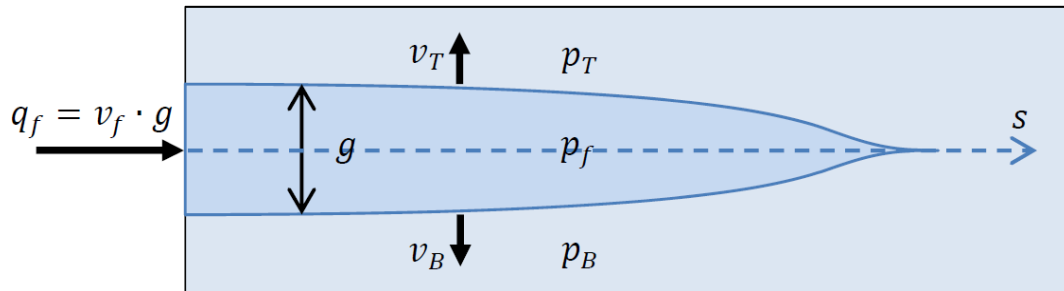


Figure 2. Overview of fluid flow during fracture and its penetration into the surrounding porous medium.

Assuming that hydraulic fracturing fluid prevents the fluid from leaking into the formation by creating a filter cake, this means $V_T = V_B = 0$. Therefore, the continuity equation can be written as follows:

$$g = \frac{\partial}{\partial s} \left(\frac{g^3}{12\mu_f} \frac{\partial p_f}{\partial s} \right) \quad (15)$$

Nevertheless, if the hydraulic fracturing fluid can penetrate the porous media, it is assumed that:

$$\begin{aligned} V_T &= c_T(p_f - p_T) \\ V_B &= c_B(p_f - p_B) \end{aligned} \quad (16)$$

where p_T and p_B are the pore pressure of the perforated fluid at the top and bottom of the fracture, and c_T and c_B are the leakage coefficients. This model simulates the leakage of a filter layer that may accumulate and reduce the effective normal permeability of failure surfaces. Thus, the equation for hydraulic fracturing fluid flow is as follows:

$$g + c_T(p_f - p_T) + c_B(p_f - p_B) = \frac{\partial}{\partial s} \left(\frac{g^3}{12\mu_f} \frac{\partial p_f}{\partial s} \right) \quad (17)$$

Each of the numerical methods have some advantages and disadvantages, which should be taken into consideration for each specific case. It can be said that in many numerical models, recognition of continuous and discontinuous environments will have a profound impact on the modeling processes. Therefore, it is necessary to use influential factors to identify different types of environments. In this study, hydraulic fracturing operations were modeled using the finite element method to compare with the real fracturing processes. In other words, a three-dimensional numerical model was used to simultaneously consider the solid mechanical equations, fluids, and fracture geometry, as well as pressures during operation.

2.2. Numerical Procedure

One of the advantages of the numerical method is that after making the model, it is possible to check all the parameters affecting each process. Therefore, in this section, first, the initial results of the base model such as fracture opening profile, fluid leakage rate and intra-fracture fluid pressure changes were presented. A complete analysis of Abacus software is usually made up of three stages: the preprocessing stage, the processing stage, and the post-processing stage. In the preprocessing step of the problem of geometric modeling, the dissection of the model is done using the appropriate element and the application of loading and boundary conditions according to the methods used by the finite elements. After completing the preprocessing steps, the created model can be sent to

Abacus program processors. At the end of the preprocessing step, the model is sent to the processing unit for analysis of the finite element component. Post-processing software can be used to visualize the results. The modeling results can be displayed in the form of meters, moving images, or diagrams of changes to the desired parameter during analysis. In this paper, a three-dimensional model of an oil reservoir was constructed using the finite element method. This model represents a porous medium, so reservoir characteristics such as porosity, permeability, porous pressure, saturation percentage, and the specific gravity of individual fluid are included. The first stage of problem-solving is the geostatic stage. Since then, initial boundary conditions were assumed to balance the proposed model. Then, high-pressurized fracturing fluid was injected in the formation rock with a flow rate of 12 barrels per minute and the injection time of 30 min. A hydraulic fracture was created and eventually expanded. It is shown schematically in Figure 3.

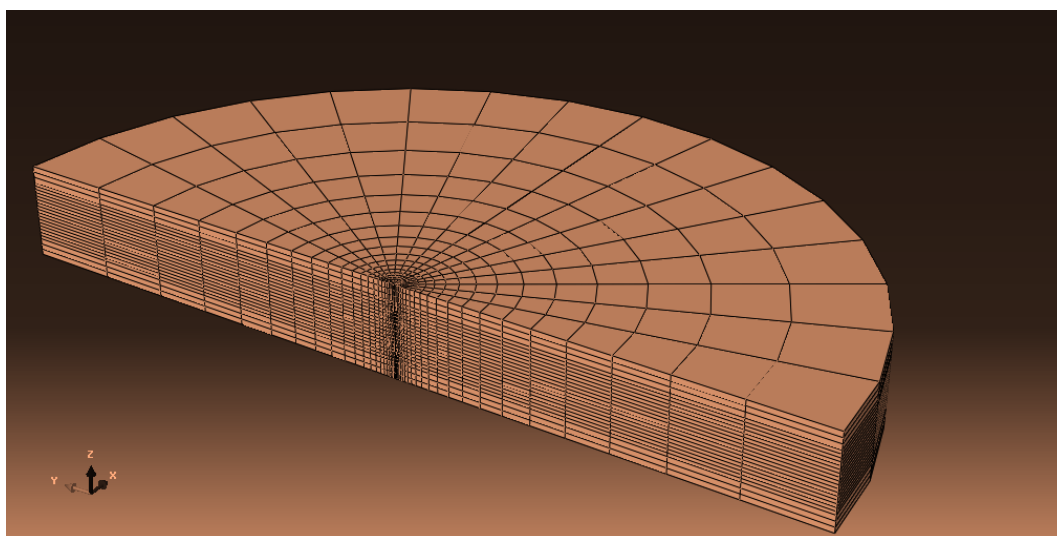


Figure 3. A three-dimensional model of an oil reservoir with finite elements.

The first step in building a model is to create the desired geometry for the problem. The dimensions of the model are in the form of a circular reservoir. Due to the lack of influence of artificial borders in the calculation process, the radius of the tank is 1000 m and its thickness is about 120 m. The diameter of the well is 0.125 m, which is modeled in order to reduce the dissolution time and to use the symmetry law. Hydraulic fracturing operations were performed at two different depths between 3104 to 2984 (Layer A) meters and 4216 to 4326 (Layer B) meters. It should be noted that the hydraulic fracturing procedure was simulated in the middle section and all the results presented in this research are specific to the central section. One of the oil reservoirs in the Bangestan oilfield in the south of Iran is used in this modeling, and its input parameters are statistically explained in Table 1. According to the field data, effective fluid flow is in the porosity of 20–25% and permeability of 20–30 mD.

Table 1. Input parameters from the Bangestan oilfield.

Parameter	Value	Unit
Young Modulus (E)	GPa	40.12
Poisson's ratio (γ)	Dimensionless	0.3
Porosity (\emptyset)	%	15
Permeability (k)	mD	12
Rock Density (ρ_b)	kg/m ³	2500
Fluid Density (ρ_o)	kg/m ³	1120
Tension Strength (T_o)	MPa	7.5

3. Results

3.1. Volumetric Flux Rate

The injectable fluid leakage rate is one of the most important things during the designation of a hydraulic operation. Calculating the exact amount of fluid leakage rate requires solving of the equilibrium mass balance equations and making accurate information about the rock and fluid. However, considering that the fluid can enter the formation from the inside of the fracture, volumetric flux rate changes over the injection time. It is plotted for two different layers in Figure 4. As can be seen in Figure 4, the amount of volumetric flux rate can be divided into three time stages. In the first stage, the volumetric flux rate is accompanied by a sudden increase, and then, in the second stage, the volumetric flux rate decreases. In the last stage, it reaches a plateau. The first two stages are caused by the creation of the first level of fracture. Fluid would be lost in the formation. In the third stage, the fluid has a constant volumetric flux rate into the formation.

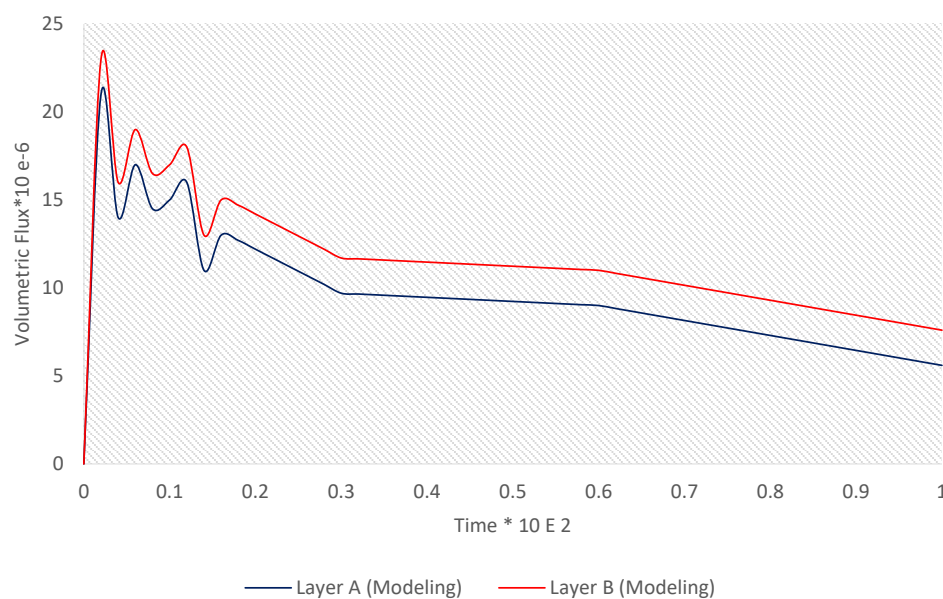


Figure 4. Volumetric flux rate versus time for two different layers.

According to Figure 4, the pore volume injection was increased dramatically as it needs to open the fractures or create new fractures [36].

3.2. Pressure–Time Curve

As can be seen in Figure 5, the pressure was plotted versus time to consider the effect of pressure versus time through fracture propagation. It is observed that the maximum amount of break pressure for layers A and B is 75 and 80 MPa, respectively. The minimum pressure at the end of fracture expansion is measured 55 and 64 MPa for layers A and B, respectively. In the first steps of fracturing, there is a dramatic increase in the pressure as it is necessary to perforate the cohesive cracks. Since then, it is decreased gradually until the formation is completely ruptured. To validate the model, a set of field data for the studied field is provided and as can be seen from the pressure drop figure, the developed model is in good agreement with the field data.

3.3. Fracture Opening Profile

Fracture opening is one of the essential outputs in which fracture width changes can be obtained before and after fluid injection. The success rate of the hydraulic fracturing process can be justified in this step. Fracture width is directly related to the permeability and flow rate of the hydrocarbon

fluid flow inside the formation. It is clear that increasing the width of the fracture and keeping it stable after the injection by propane can play an instrumental role in increasing the permeability and fluid flow. Hence, the oil well production rate is affected accordingly. Figure 5 indicates the opening of the fracture at the injection point at different times and along the length of the fracture at a depth of 1. The maximum fracture opening at the junction of the well at about 10 mm is the maximum change in the dimensions of the fracture at the end of the fracture and the middle points have a slight slope and the fracture tip at the end of the injection time. It is located 20 m from the injection point. To validate the model, a set of field data for the studied field is provided and as can be seen from the pressure drop figure, the developed model is in a good agreement with the field data. It is indicated in Figure 6.

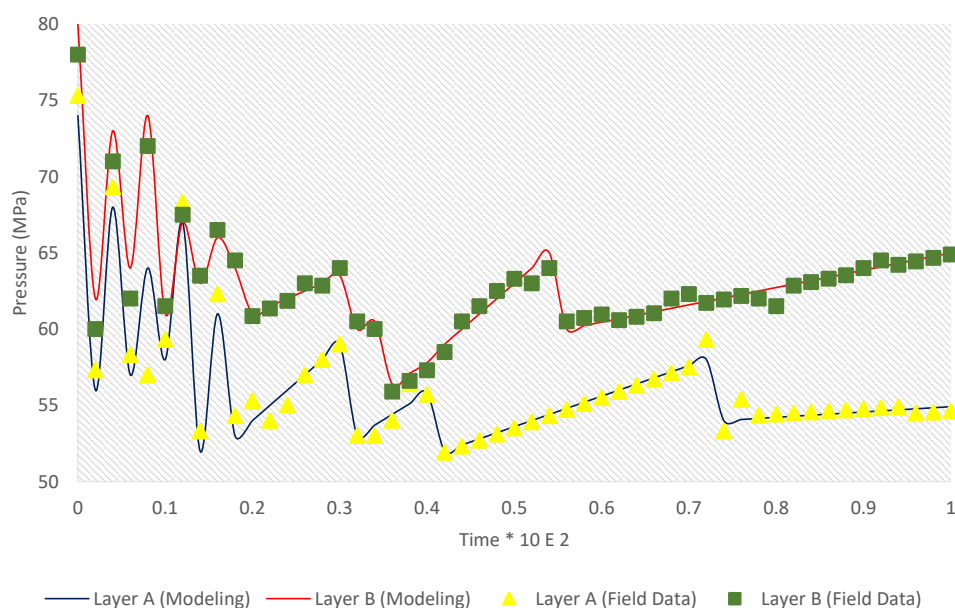


Figure 5. Pressure versus time.

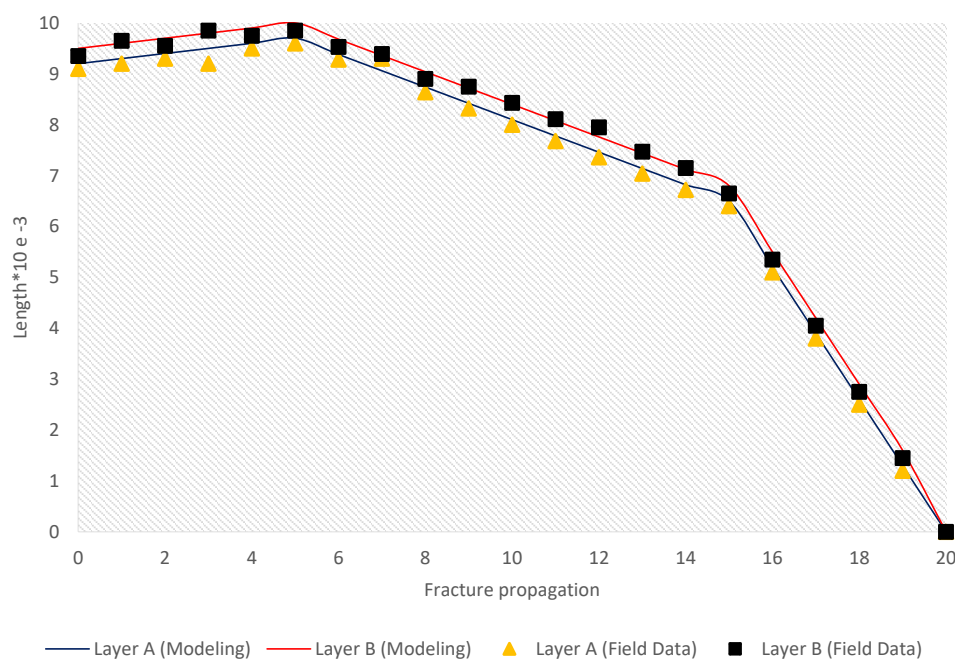


Figure 6. Fracture opening profile.

The fracture opening profile before and after the fluid injection are shown in Figures 7–10 for layers A and B. In fact, they represent a longitudinal profile (along the x–z plane) of the fracture opening before and after the injection. They reflect the opening position of the central part of the oil layer due to fluid injection. The value starts from 10 and 9 mm for layer B and layer A near the injection well, and it gradually decreases with distance from the well axis.

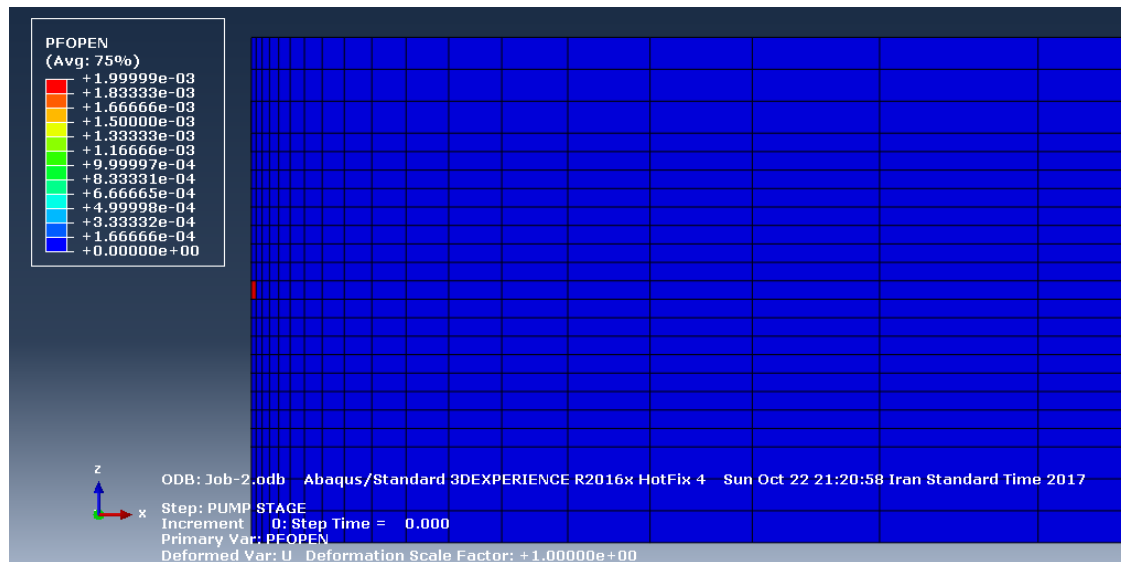


Figure 7. The fracture opening profile a longitudinal profile (along the x–z plane) before the fluid injection (Layer A).

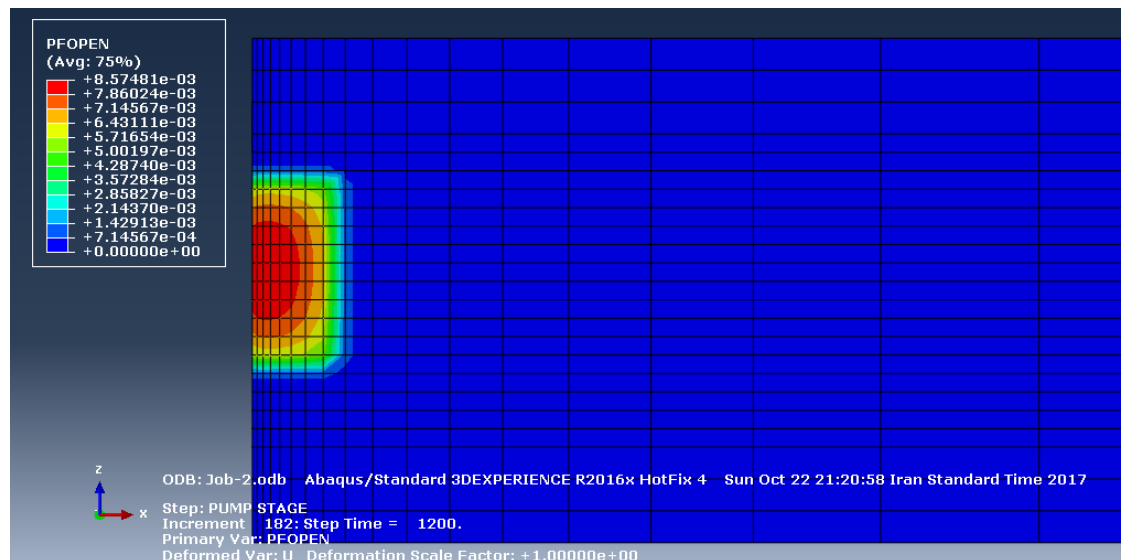


Figure 8. The fracture opening profile a longitudinal profile (along the x–z plane) after the fluid injection (Layer A).

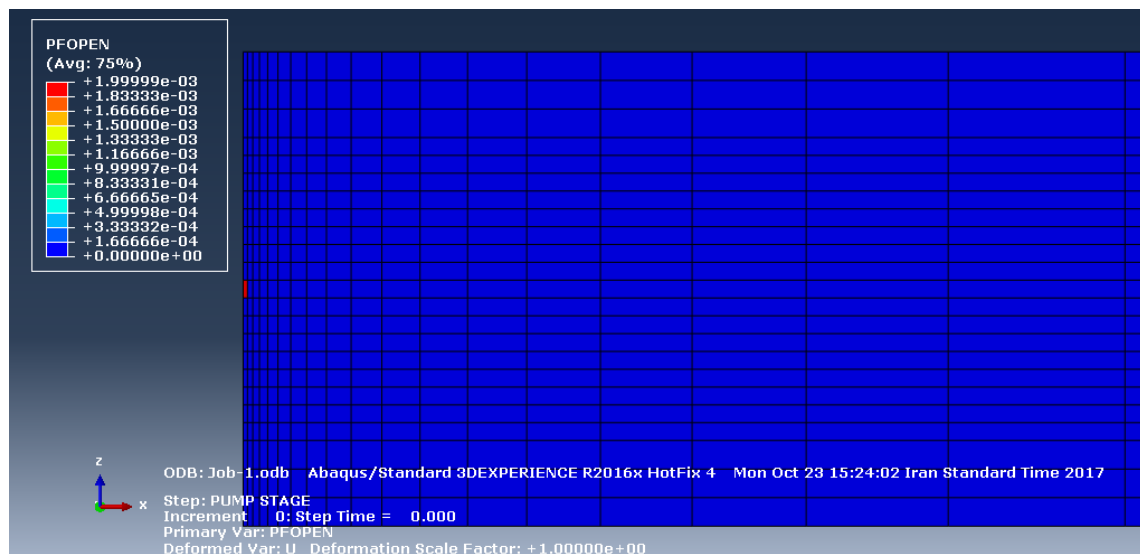


Figure 9. The fracture opening profile a longitudinal profile (along the x–z plane) before the fluid injection (Layer B).

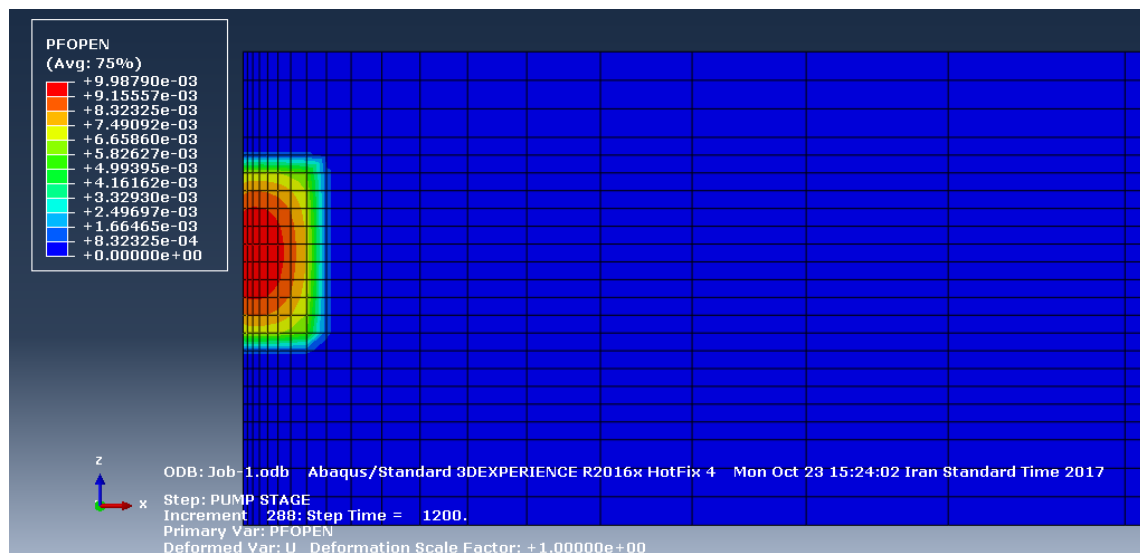


Figure 10. The fracture opening profile a longitudinal profile (along the x–z plane) after the fluid injection (Layer B).

3.4. Pressure Drop through Fractures

Figure 11 shows a diagram of the fluid pressure changes within the fracture along the length of the fracture to complete the injection operation. For Layer A, the amount of pressure inside the fracture is 53 MPa, while the fluid pressure inside the fracture for Layer B is 64 MPa. To validate the model, a set of field data for the studied field is provided and as can be seen from the pressure drop figure, the developed model is in a good agreement with the field data.

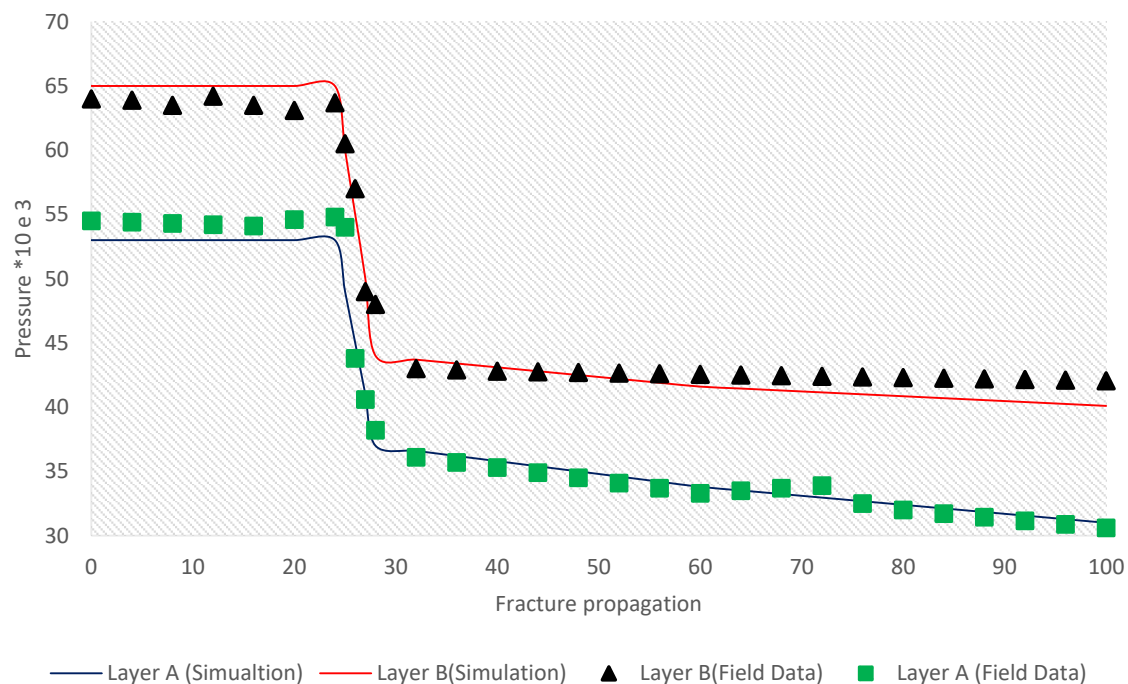


Figure 11. Pressure drop through fractures.

4. Discussion

Due to the complexity of analytical methods and their time-consuming property to address engineering issues, numerical methods have always been taken into consideration. The finite element method (henceforth; FEM) is one of the efficient and optimum solutions in engineering aspects. Generally speaking, regarding the fractures' behavior that significantly influenced the hydraulic fracturing performances, fracturing models such as cohesive crack zone and linear elastic fracturing models are investigated in this paper. The geomechanical limitations of this model that are considered in the developed model are as follows:

- ✓ It is assumed that the distribution of different properties, such as porosity, permeability, and saturation, is uniform in the reservoir.
- ✓ The rock mechanical behavior is assumed elastoplastic, and it is assumed that the layers are continuous without any cracks and natural fractures, in which finite element method can be used.
- ✓ Moreover, due to the importance of the top and bottom reservoir layers and the expansion or non-expansion of hydraulic fractures in them, sufficient information about the involved layers is also required.

Abacus can solve a wide range of problems from a relatively simple linear analysis to very complex nonlinear analyzes. This software includes an extensive library of elements that can model any type of geometries vertically. The software also includes an extensive list of material behavior models that can simulate the behavior of most engineering materials. Furthermore, issues that have multiple components and different materials can be defined by defining the geometry of each component and assigning its constituent materials, and then, defining the interaction between them.

The presence of porous rock spaces and fluid through them can significantly simplify the simulation processes, and would be more reliable for field data measurements. Moreover, alteration of geomechanical characteristics during the injection and production performances could be taken into consideration. Wang et al. [37] proposed a numerical method coupled with the solid–fluid to model the hydraulic fracture propagation in the orthotropic formations by the extended finite element method. They investigated the fluid flow and rock deformation interaction through the fractures,

hydraulic fracture propagation and maximum circumferential tensile stress criterion that is modified accordingly in their model. They concluded that if an angle had existed between the orthotropic material axes and initial fracture direction, the hydraulic fracture would have deviated from the straight path. This angle would be changed by the material angle variations, which had caused an increase in Young's Modulus ratio [37]. In this model, the poroelastic theory is used to consider geomechanical characteristics of the hydrocarbon formation, such as fluid flow in the pore spaces, was developed. It is concluded that during the production operation from the hydrocarbon reservoir, internal fluid pressure decreases. It has caused an increase in effective stresses that are applied to the formation. This phenomenon was discussed by Wang et al. [37] as Young's modulus ratio increases. This is indicated in Figure 6 that the fracture deviation through the length of the porous media is related to the oriented angle, which has caused an increase in Young's Modulus ratio. Moreover, Liu et al. [36] developed an extended finite element framework to consider the propagation of hydraulic fractures containing the poroelastic behavior between fluid flow and the bulk formation, and how to model their interaction [36]. According to the results of this paper, the interaction between fluid and bulk formation, rock pore spaces would be reduced or might be occupied by the solid particles during the propagation of the fracture that is discussed by Liu et al. [36]. By mobilizing the fracture fluid through fractures, its volume has decreased slightly, and in the last steps, it reached a plateau. This concept is considered by Liu et al. [36] by developing an extended finite element framework to investigate the interaction between bulk formation and fluid flow.

One of the essential things in fractures modeling is to study the different fracture creation methods that were investigated by Ji [38] and Guo [39]. It is possible to use fracture volume and consider such assumptions of fracture shape, length and width of the fracture, and pressure distribution by having assumptions such as the shape of the fracture, the distribution of pressure, and the width and length of the fracture [38,39]. In the proposed models, fracture expansion is only one direction perpendicular to the minimum principal stress, while in this paper, a longitudinal profile (along the x - z plane) of the fracture opening profile was represented. Feng et al. [40] investigated a multi-stage fractured horizontal well as a numerical model to calculate fracture pressure drop by the consideration of dynamic fracture closure, matrix permeability change, and threshold pressure gradient for one well that is in accordance of the result in this section [40]. However, in this paper, it was modeled for two different layers that would be expandable for more layers. Moreover, physical-mechanical reservoir characteristics could be considered simultaneously.

Gao et al. [41] proposed a developed numerical model based on the cohesive zone method and extended finite element method to consider the impact of hydraulic fracturing propagation during operation performances. In this model, leak-off, propagation, hydraulic fracturing initiation, rock deformation, and fracturing fluid flow was modeled simultaneously. According to their results, fracture propagation is utterly dependent on the existence of injection wells during operational performances, and production wells did not play a substantial role in the length of the fractures. Furthermore, higher pore pressures will be needed for injecting processes than production processes during the hydraulic fracturing operations [41]. According to the results of this paper, during the injection of high-pressure fluid into the rock pore spaces, the effective stresses will reduce, and this event will cause tensile failure in the rock, which is discussed in Gao et al. [41].

Thereby, in this paper, a three-dimensional numerical model was developed to simultaneously consider the mechanical equations of solids, fluids and fractures as a longitudinal profile along the (x - z) plane. To do this, Abacus software was used as a multi-objective program to model the hydraulic fracturing processes by assuming limitations and solving the governing equations. Moreover, physical and mechanical reservoir properties in porous media according to the finite element method were considered in the model. Finally, this model is numerically efficient as it can be administered for computational cost-effective and different scales to provide sophisticated numerical computing of hydrodynamic fluid flow through porous media and propagation of fracture versus pressure and time for different layers.

5. Conclusions

Abacus software was based on the finite element method was used to investigate the hydraulic fracturing operations in an oil reservoir field in the Bangestan field in the south of Iran. In this model, the theory of adhesive crack model with tensile law separation of finite elements and symmetry law have been used to create and expand fractures within the three-dimensional pore-elastic model. The main conclusions of this paper are as follows:

The maximum fracture opening at the well connection for Layer A is about 9 mm, and for Layer B is about 10 mm.

The most considerable change in fracture dimensions is achieved at the end of the fracture, and the midpoints have a slight slope.

The fracture tip is located at the end of the injection time at a distance of 20 m from the injection site.

It is concluded that the amount of pressure decreases with distance from the injection site and eventually reaches the initial permeable pressure of the environment. For Layer A, the amount of pressure inside the fracture is 53 MPa, while the fluid pressure inside the fracture for depth 2 is 65 MPa.

For future studies, it is suggested that sensitivity analysis will be performed on how different geomechanical parameters affect fracture geometry and operating pressures. Moreover, it is recommended that the results of numerical simulation be compared with more actual field data obtained from the operational performances if the operational and actual data from the oil reservoir are available to expand the model to more different wells. Finally, if the perforation data are accessible, this model would be adopted to this issue and would provide exciting results for petroleum industries.

Author Contributions: S.S.; Data curation, formal analysis, writing—original draft and investigation. M.Z.; methodology and project administration. W.L.; Visualization. A.D.; Writing—review and editing, supervision, and validation. All authors have read and agreed to the published version of the manuscript.

Funding: This research received no external funding.

Acknowledgments: This work was supported by 2019 Anhui University Humanities And Social Science Research Key Project (SK2019A0526), 2017 Annual Outstanding Youth Backbone Talents Domestic Visiting Study Project of Higher Education Institution in Anhui province (gxhx2017127), Start Project of Scientific Research by Professors and Doctors of Suzhou University (2015JB11), and the Massive Open Online Courses (MOOC) of the Provincial Quality Project of Anhui Provincial Higher Education Institutions (2016mooc301).

Conflicts of Interest: The authors declare no conflict of interest.

References

1. Mahoney, R.P.; Soane, D.S.; Herring, M.K.; Kincaid, K.P. Self-Suspending Proppants for Hydraulic Fracturing. U.S. Patents Application No. 9,315,721 B2, 19 April 2016.
2. Rabbani, E.; Davarpanah, A.; Memariani, M. An experimental study of acidizing operation performances on the wellbore productivity index enhancement. *J. Pet. Explor. Prod. Technol.* **2018**, *8*, 1243–1253.
3. Vengosh, A.; Kondash, A.; Harkness, J.; Lauer, N.; Warner, N.; Darrah, T.H. The geochemistry of hydraulic fracturing fluids. *Procedia Earth Planet. Sci.* **2017**, *17*, 21–24. [[CrossRef](#)]
4. Davarpanah, A. A feasible visual investigation for associative foam >\polymer injectivity performances in the oil recovery enhancement. *Eur. Polym. J.* **2018**, *105*, 405–411. [[CrossRef](#)]
5. Davarpanah, A.; Mirshekari, B. Experimental study and field application of appropriate selective calculation methods in gas lift design. *Pet. Res.* **2018**, *3*, 239–247. [[CrossRef](#)]
6. Davarpanah, A.; Mirshekari, B. A mathematical model to evaluate the polymer flooding performances. *Energy Rep.* **2019**, *5*, 1651–1657. [[CrossRef](#)]
7. Davarpanah, A.; Mirshekari, B.; Jafari Behbahani, T.; Hemmati, M. Integrated production logging tools approach for convenient experimental individual layer permeability measurements in a multi-layered fractured reservoir. *J. Pet. Explor. Prod. Technol.* **2018**, *8*, 743–751. [[CrossRef](#)]
8. Pan, F.; Zhang, Z.; Zhang, X.; Davarpanah, A. Impact of anionic and cationic surfactants interfacial tension on the oil recovery enhancement. *Powder Technol.* **2020**, *373*, 93–98. [[CrossRef](#)]
9. Guo, J.; Luo, B.; Lu, C.; Lai, J.; Ren, J. Numerical investigation of hydraulic fracture propagation in a layered reservoir using the cohesive zone method. *Eng. Fract. Mech.* **2017**, *186*, 195–207. [[CrossRef](#)]

10. Zhang, Y.; Zhang, J.; Yuan, B.; Yin, S. In-situ stresses controlling hydraulic fracture propagation and fracture breakdown pressure. *J. Pet. Sci. Eng.* **2018**, *164*, 164–173. [\[CrossRef\]](#)
11. Zeng, Q.-D.; Yao, J.; Shao, J. Numerical study of hydraulic fracture propagation accounting for rock anisotropy. *J. Pet. Sci. Eng.* **2018**, *160*, 422–432. [\[CrossRef\]](#)
12. Davarpanah, A. Feasible analysis of reusing flowback produced water in the operational performances of oil reservoirs. *Environ. Sci. Pollut. Res.* **2018**, *25*, 35387–35395. [\[CrossRef\]](#) [\[PubMed\]](#)
13. Davarpanah, A.; Shirmohammadi, R.; Mirshekari, B.; Aslani, A. Analysis of hydraulic fracturing techniques: Hybrid fuzzy approaches. *Arab. J. Geosci.* **2019**, *12*, 402. [\[CrossRef\]](#)
14. Missimer, T.M.; Maliva, R.G. Hydraulic Fracturing in Southern Florida: A Critical Analysis of Potential Environmental Impacts. *Nat. Resour. Res.* **2020**, 1–27. [\[CrossRef\]](#)
15. Wu, Z. Analytical Fracture Models for Overall Hydraulic Fracturing Reservoirs. *Int. J. Oil Gas Coal Eng.* **2019**, *7*, 13. [\[CrossRef\]](#)
16. Davarpanah, A.; Mirshekari, B. Mathematical modeling of injectivity damage with oil droplets in the waste produced water re-injection of the linear flow. *Eur. Phys. J. Plus* **2019**, *134*, 180. [\[CrossRef\]](#)
17. Flekkøy, E.G.; Målthe-Sørenssen, A.; Jamtveit, B. Modeling hydrofracture. *J. Geophys. Res. Solid Earth* **2002**, *107*, ECV 1-1–ECV 1-11. [\[CrossRef\]](#)
18. Yan, C.; Zheng, H. FDEM-flow3D: A 3D hydro-mechanical coupled model considering the pore seepage of rock matrix for simulating three-dimensional hydraulic fracturing. *Comput. Geotech.* **2017**, *81*, 212–228. [\[CrossRef\]](#)
19. Fu, W.; Savitski, A.A.; Damjanac, B.; Bunger, A.P. Three-dimensional lattice simulation of hydraulic fracture interaction with natural fractures. *Comput. Geotech.* **2019**, *107*, 214–234. [\[CrossRef\]](#)
20. Lecampion, B.; Bunger, A.; Zhang, X. Numerical methods for hydraulic fracture propagation: A review of recent trends. *J. Nat. Gas Sci. Eng.* **2018**, *49*, 66–83. [\[CrossRef\]](#)
21. Brandes, C.; Tanner, D.C. Chapter 2—Fault mechanics and earthquakes. In *Understanding Faults*; Tanner, D., Brandes, C., Eds.; Elsevier: Amsterdam, The Netherlands, 2020; pp. 11–80. [\[CrossRef\]](#)
22. Al-Busaidi, A.; Hazzard, J.F.; Young, R.P. Distinct element modeling of hydraulically fractured Lac du Bonnet granite. *J. Geophys. Res. Solid Earth* **2005**, *110*. [\[CrossRef\]](#)
23. Ghani, I.; Koehn, D.; Toussaint, R.; Passchier, C.W. Dynamic Development of Hydrofracture. *Pure Appl. Geophys.* **2013**, *170*, 1685–1703. [\[CrossRef\]](#)
24. Kumari, W.; Ranjith, P.; Perera, M.; Li, X.; Li, L.; Chen, B.; Isaka, B.A.; De Silva, V. Hydraulic fracturing under high temperature and pressure conditions with micro CT applications: Geothermal energy from hot dry rocks. *Fuel* **2018**, *230*, 138–154. [\[CrossRef\]](#)
25. Sarvaramini, E.; Dusseault, M.B.; Gracie, R. Characterizing the stimulated reservoir volume during hydraulic fracturing-connecting the pressure fall-off phase to the geomechanics of fracturing. *J. Appl. Mech.* **2018**, *85*, 101006. [\[CrossRef\]](#)
26. Haghi, A.; Chalaturnyk, R.; Ghobadi, H. The state of stress in SW Iran and implications for hydraulic fracturing of a naturally fractured carbonate reservoir. *Int. J. Rock Mech. Min. Sci.* **2018**, *105*, 28–43. [\[CrossRef\]](#)
27. Jenkins, A.; Fathi, E.; Belyadi, F. Stress field behavior induced by hydraulic fracture in shale reservoirs: A practical view on cluster spacing. *J. Nat. Gas Sci. Eng.* **2017**, *48*, 186–196. [\[CrossRef\]](#)
28. Narasingam, A.; Siddhamshetty, P.; Sang-II Kwon, J. Temporal clustering for order reduction of nonlinear parabolic PDE systems with time-dependent spatial domains: Application to a hydraulic fracturing process. *AIChE J.* **2017**, *63*, 3818–3831. [\[CrossRef\]](#)
29. Karakin, A.; Ramazanov, M.; Borisov, V. Incompletely Coupled Equations of Hydraulic Fracturing. *Math. Models Comput. Simul.* **2018**, *10*, 45–58. [\[CrossRef\]](#)
30. Liu, C.; Shen, Z.; Gan, L.; Jin, T.; Zhang, H.; Liu, D. A hybrid finite volume and extended finite element method for hydraulic fracturing with cohesive crack propagation in quasi-brittle materials. *Materials* **2018**, *11*, 1921. [\[CrossRef\]](#)
31. Zhang, F.; Damjanac, B.; Maxwell, S. Investigating Hydraulic Fracturing Complexity in Naturally Fractured Rock Masses Using Fully Coupled Multiscale Numerical Modeling. *Rock Mech. Rock Eng.* **2019**, *52*, 5137–5160. [\[CrossRef\]](#)
32. Zheng, H.; Pu, C.; Sun, C. Numerical investigation on the hydraulic fracture propagation based on combined finite-discrete element method. *J. Struct. Geol.* **2020**, *130*, 103926. [\[CrossRef\]](#)

33. He, B.; Schuler, L.; Newell, P. A numerical-homogenization based phase-field fracture modeling of linear elastic heterogeneous porous media. *Comput. Mater. Sci.* **2020**, *176*, 109519. [[CrossRef](#)]
34. Alotaibi, T.E.; Landis, C.M.; AlTammar, M.J. Phase-Field Modeling of Hydraulic Fracture Propagation in Mechanically Heterogeneous Formations. In Proceedings of the International Petroleum Technology Conference, Dhahran, Saudi Arabia, 13 January 2020; p. 15.
35. Zielonka, M.G.; Searles, K.H.; Ning, J.; Buechler, S.R. Development and validation of fully-coupled hydraulic fracturing simulation capabilities. In Proceedings of the SIMULIA community conference, SCC2014, Providence, RI, USA, 19–22 May 2014; pp. 19–21.
36. Liu, F.; Gordon, P.A.; Valiveti, D.M. Modeling competing hydraulic fracture propagation with the extended finite element method. *Acta Geotech.* **2018**, *13*, 243–265. [[CrossRef](#)]
37. Wang, X.; Shi, F.; Liu, H.; Wu, H. Numerical simulation of hydraulic fracturing in orthotropic formation based on the extended finite element method. *J. Nat. Gas Sci. Eng.* **2016**, *33*, 56–69. [[CrossRef](#)]
38. Ji, L. Modeling Hydraulic Fracturing Fully Coupled with Reservoir Geomechanical Simulation. Ph.D. Thesis, University of Calgary, Calgary, AB, Canada, 2008.
39. Guo, B. *Petroleum Production Engineering, a Computer-Assisted Approach*; Elsevier: Amsterdam, The Netherlands, 2011.
40. Feng, Q.; Jiang, Z.; Wang, S.; Zhang, G.; Qin, Y.; Xu, S.; Zhang, W. Optimization of reasonable production pressure drop of multi-stage fractured horizontal wells in tight oil reservoirs. *J. Pet. Explor. Prod. Technol.* **2019**, *9*, 1943–1951. [[CrossRef](#)]
41. Gao, Q.; Cheng, Y.; Han, S.; Yan, C.; Jiang, L. Numerical modeling of hydraulic fracture propagation behaviors influenced by pre-existing injection and production wells. *J. Pet. Sci. Eng.* **2019**, *172*, 976–987. [[CrossRef](#)]



© 2020 by the authors. Licensee MDPI, Basel, Switzerland. This article is an open access article distributed under the terms and conditions of the Creative Commons Attribution (CC BY) license (<http://creativecommons.org/licenses/by/4.0/>).